Abolishing storage lipids induces protein misfolding and stress responses in Yarrowia lipolytica

Downloaded from: https://research.chalmers.se, 2026-04-05 22:36 UTC

Citation for the original published paper (version of record):

Zaghen, S., Konzock, O., Fu, J. et al (2023). Abolishing storage lipids induces protein misfolding and stress responses in Yarrowia lipolytica. Journal of Industrial Microbiology and Biotechnology, 50(1). http://dx.doi.org/10.1093/jimb/kuad031

N.B. When citing this work, cite the original published paper.

research.chalmers.se offers the possibility of retrieving research publications produced at Chalmers University of Technology. It covers all kind of research output: articles, dissertations, conference papers, reports etc. since 2004. research.chalmers.se is administrated and maintained by Chalmers Library

(article starts on next page)

Journal of Industrial Microbiology and Biotechnology, 2023, 50, kuad031
https://doi.org/10.1093/jimb/kuad031
Advance access publication date: 23 September 2023
Applied Genomics & Systems Biotechnology—Original Paper

Abolishing storage lipids induces protein misfolding and stress responses in *Yarrowia lipolytica*

Simone Zaghen[1,†], Oliver Konzock[1,†], Jing Fu[1], Eduard J. Kerkhoven[1,2,3]

[1]Division of Systems and Synthetic Biology, Department of Life Sciences, Chalmers University of Technology, Göteborg, Sweden
[2]SciLifeLab, Chalmers University of Technology, Göteborg 412 96, Sweden
[3]Novo Nordisk Foundation Center for Biosustainability, Technical University of Denmark, 2800 Lyngby, Denmark
Correspondence should be addressed to: Eduard J. Kerkhoven at eduardk@chalmers.se
[†]These authors contributed equally.

Abstract: *Yarrowia lipolytica* naturally saves excess carbon as storage lipids. Engineering efforts allow redirecting the high precursor flux required for lipid synthesis toward added-value chemicals such as polyketides, flavonoids, and terpenoids. To redirect precursor flux from storage lipids to other products, four genes involved in triacylglycerol and sterol ester synthesis (*DGA1*, *DGA2*, *LRO1*, and *ARE1*) can be deleted. To elucidate the effect of the deletions on cell physiology and regulation, we performed chemostat cultivations under carbon and nitrogen limitations, followed by transcriptome analysis. We found that storage lipid-free cells show an enrichment of the unfolded protein response, and several biological processes related to protein refolding and degradation are enriched. Additionally, storage lipid-free cells show an altered lipid class distribution with an abundance of potentially cytotoxic free fatty acids under nitrogen limitation. Our findings not only highlight the importance of lipid metabolism on cell physiology and proteostasis, but can also aid the development of improved chassy strains of *Y. lipolytica* for commodity chemical production.

Keywords: Q4 strain, Fat free *Yarrowia lipolytica*, Lipid classes, Fatty acid toxicity, Lipotoxicity

Graphical abstract

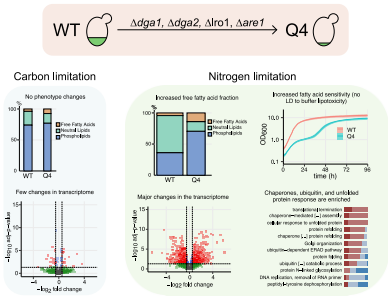

Engineering *Yarrowia lipolytica* to redirect carbon flux from storage lipids to valuable chemicals alters cell physiology, emphasizing the significance of lipid metabolism in proteostasis and suggesting areas of improvement for future strains.

Introduction

The initial interest in the oleaginous yeast *Yarrowia lipolytica* was focused on its ability to secrete lipases and its lipid production capacity (Nicaud, 2012). *Yarrowia lipolytica* can produce up to 80% of its dry weight as lipids thanks to metabolic engineering and media optimization (Friedlander et al., 2016). The lipids produced by *Y. lipolytica* find applications as biofuels, nutritional supplements, cosmetic additives, and vegetable oil substitutes (Gonçalves et al., 2014; Zeng et al., 2018). Lipid biosynthesis requires high amounts of acetyl-CoA. High amounts of acetyl-CoA can be redirected from lipid production to commodity and added-value chemicals production through metabolic engineering. Consequently, the interest in *Y. lipolytica* started to encompass the production of flavonoids (naringenin [Palmer et al., 2020], eriodictyol [Lv et al., 2019], and taxifolin [Lv et al., 2019]), polyketides (triacetic lactone [Markham et al., 2018] and resveratrol [Palmer et al., 2020]), and terpenoids (lycopene [Matthäus et al., 2014], β-carotene [Gao et al., 2017], and limonene [Cheng et al., 2019]).

Under nitrogen limitation (N-lim) *Y. lipolytica* has a high acetyl-CoA flux, which is directed toward lipid accumulation (Beopoulos et al., 2008; Kerkhoven et al., 2016). Under N-lim, the activity of the adenosine monophosphate deaminase (AMP deaminase) is increased, resulting in low AMP levels. Low AMP levels inhibit isocitrate dehydrogenase in the tricarboxylic acid cycle, resulting in citrate accumulation in the mitochondria.

Received: August 15, 2023. **Accepted:** September 19, 2023.
© The Author(s) 2023. Published by Oxford University Press on behalf of Society of Industrial Microbiology and Biotechnology. This is an Open Access article distributed under the terms of the Creative Commons Attribution License (https://creativecommons.org/licenses/by/4.0/), which permits unrestricted reuse, distribution, and reproduction in any medium, provided the original work is properly cited.

Downloaded from https://academic.oup.com/jimb/article/50/1/kuad031/7281721 by guest on 07 November 2023

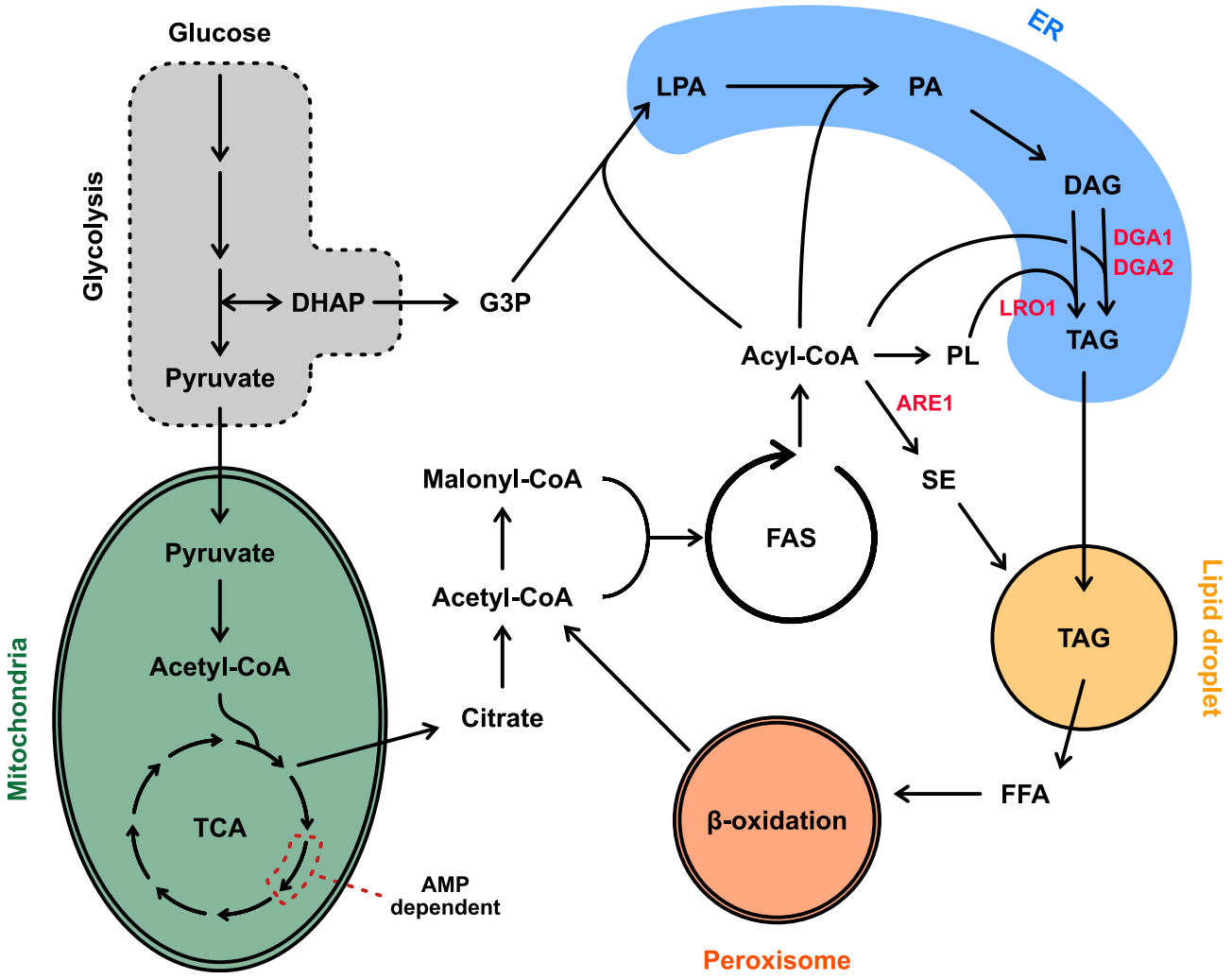

Fig. 1. Overview of lipid metabolism in Yarrowia *lipolytica*. In red are the genes that have been deleted in JFYL007 (also referred to as the Q4 strain) to abolish storage lipid accumulation. Adapted from Konzock (2022). DAG = diacylglycerol; DHAP = dihydroxyacetone phosphate; ER = endoplasmic reticulum; FAS = fatty acid synthase; FFA = free fatty acid; G3P = glyceraldehyde 3-phosphate; LPA = lysophosphatidic acid; PA = phosphatidic acid; PL = phospholipid; SE = sterol ester; TAG = triacylglycerol; TCA = tricarboxylic acid cycle.

Mitochondrial citrate is shuttled into the cytosol by the malate/citrate transferase, where it is cleaved into acetyl-CoA by the ATP-citrate lyase. Acetyl-CoA can enter lipid metabolism and can be incorporated into storage lipids. Storage lipids in *Y. lipolytica* are mainly formed by triacylglycerols (TAGs) and small amounts (<5%) of sterol esters (SE) (Beopoulos et al., 2012). Storage lipids are produced on the endoplasmic reticulum (ER) membrane and accumulate in lipid droplets (LDs) (Fig. 1; Sandager et al., 2002; Wang et al., 2020).

Storage lipid production can be prevented by deleting four genes, namely *DGA1* (YALI1_E38810g), *DGA2* (YALI1_D10264g), *LRO1* (YALI1_E20049g), and *ARE1* (YALI1_F09747g) (Beopoulos et al., 2012). *DGA1* and *DGA2* catalyse the final step of TAG formation and use acyl-CoA as a substrate to convert diacylglycerols (DGAs) into TAGs (Athenstaedt, 2011; Beopoulos et al., 2012). *DGA2* has also been reported to affect the size and morphology of LDs (Beopoulos et al., 2012). *LRO1* codes for a TAG synthase that is acyl-CoA-independent and uses phospholipids (PL) as acyl-donors to convert DAGs into TAGs (Athenstaedt, 2011). The Are1p of *Y. lipolytica* is essential for sterol esterification, as deletion of the encoding gene (*ARE1*) completely abolished SE synthesis (Beopoulos et al., 2012). Decreasing or inhibiting storage lipid accumulation has been shown to increase the production of added-value and commodity chemicals. Shi et al. (2021) showed that deleting *DGA1* and *DGA2* increases β-farnesene titres by 56%. Fu et al. (2023) showed that deleting *DGA1*, *DGA2*, *LRO1*, and *ARE1* increases cis-aconitate by 34% and almost doubles itaconic acid titres.

A *Y. lipolytica* strain carrying *DGA1*, *DGA2*, *LRO1*, and *ARE1* deletions (referred to as the Q4 strain) lacks storage lipid accumulation (Beopoulos et al., 2012; Poorinmohammad et al., 2022). While abolishing storage lipid accumulation is a justifiable strategy to increase the production of desired chemicals in *Y. lipolytica*, the consequences on cell physiology and regulation have not been investigated yet. To elucidate the effect of abolishing storage lipid synthesis, we performed chemostat cultivations on the wild-type strain and the Q4 strain under both carbon limitation (C-lim, C/N ratio 3) and nitrogen limitation (N-lim, C/N ratio 116). We monitored physiological parameters, including the abundance, composition, and class distribution of lipids, and we performed transcriptome analysis to assess how the deletions affect cell regulation and homeostasis.

Downloaded from https://academic.oup.com/jimb/article/50/1/kuad031/7281721 by guest on 07 November 2023

Results

Gene Deletions Affect Cell Physiology and Lipid Chain Composition in N-lim

Nutrient limitation has a major impact on gene expression in *Y. lipolytica* (Hapeta et al., 2020), and under N-lim, high flux through acetyl-CoA enables lipid accumulation (Beopoulos et al., 2008; Kerkhoven et al., 2016). To select suitable C/N ratios for chemostat fermentations, we performed shake-flask cultivations with different C/N ratios. We grew *Y. lipolytica* in media with varying glucose concentrations while maintaining the same nitrogen concentration to test C/N ratios between 1.45 and 20 and measured the OD_{600} after 72 hr. Based on the results (Supplementary Fig. 1), we selected a C/N ratio of 3 (C-lim, lipid accumulation not stimulated) for carbon limitation. Based on literature, we selected a C/N ratio of 116 (N-lim, lipid accumulation stimulated) for nitrogen limitation (Poorinmohammad et al., 2022).

To assess if cell physiology changes are related to (i) gene deletions, (ii) the C/N ratio, or (iii) a combination of both factors, we cultivated *Y. lipolytica* in chemostats under N-lim and C-lim. The pH-controlled chemostat fermentations were performed on OKYL029, displaying wild-type lipid phenotype, and on JFYL007, referred to as Q4, carrying four lipid-gene deletions (Δ*dga1*, Δ*dga2*, Δ*lro1*, and Δ*are1*), and previously used to study lipid metabolism and the role of acyltransferases (Beopoulos et al., 2012; Gajdoš et al., 2015, 2016). In both strains, hyphae formation was abolished by deleting the gene *MHY1* (Konzock & Norbeck, 2020). We picked pH-controlled chemostat cultivations to ensure a highly controlled environment that increases reproducibility. Additionally, the two strains (OKYL029 and Q4) have different growth dynamics (Supplementary Fig. 2), and a chemostat culture allows to control the growth rate by varying the dilution rate. This will reduce growth-related variability, and ensure comparable results between strains with different growth dynamics. After at least four-volume changes in chemostat fermentation, we measured the cell physiology parameters such as biomass, lipid content and composition, biomass and lipid yield, and glucose consumption.

In C-lim, cell dry weight (CDW) and lipid content were unaffected by the four deletions in the Q4 strain (Fig. 2). In C-lim, the two strains showed similar biomass yields, lipid yields, and specific glucose uptake rates (ʀ-glucose) (Fig. 2).

Even though the Q4 strain is carrying four deletions in genes involved in TAG and SE synthesis, the lipid content in the Q4 strain increased when cultivated under N-lim compared to C-lim (5.9% on N-lim and 2.3% on C-lim). Since TAG and SE synthesis are knocked out, the Q4 strain likely accumulates DAGs.

Under N-lim, both the CDW and the lipid content were negatively affected by the deletions. The CDW and the lipid content decreased by 33% and 32% in the Q4 strain compared to OKYL029, respectively. Cells grown under N-lim were dyed with BODIPY® Lipid Probe, and LDs were visible in the wild-type strain, while the Q4 strain showed no visible LDs (Supplementary Fig. 3). The lipid yield in Q4 was 37% lower than in the OKYL029 strain. Both strains showed similar biomass yields (0.44 gDCW/gGlu in Q4 and 0.48 gDCW/gGLU in OKYL029) and the same specific glucose uptake rate ($r_{glucose}$, 0.23 g/gDCWh in Q4 and 0.22 g/gDCWh in OKYL029).

Since four genes involved in lipid synthesis are deleted in the Q4 strain, we investigated their effect on the abundance and chain length of the lipids synthesized. For that, we converted the lipids to fatty acid methyl ester (FAME) and analyzed them using gas chromatography mass spectrometry (GC-MS). We found that the quadruple deletions affected the lipid composition in both C/N ratios. Regardless of the C/N ratio, the difference between strains in the C16:0 fraction is not statistically significant (p-value > .01). All the other fatty acids (FA) (C16:1, C18:0, C18:1, and C18:2) are significantly different (p-value < 0.01) between the two strains in both C/N ratios. The entity of the change is generally bigger in N-lim, but the direction of the change is the same (either more abundant in both C/N ratios or less abundant in both C/N ratios).

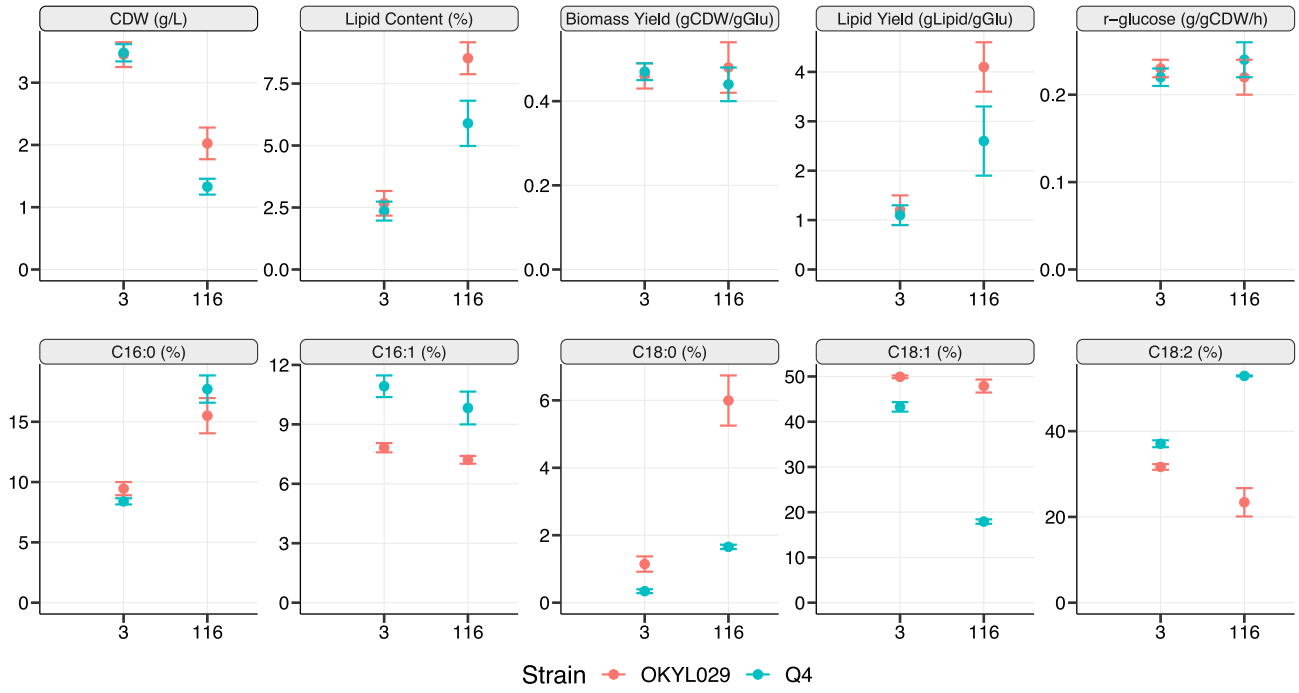

Fig. 2. Physiological and lipid composition changes of the strains OKYL029 and Q4 in C-lim (C/N ratio 3) and N-lim (C/N ratio 116). Lipid content is calculated as the percentage (%) of the lipids on the cell dry weight (CDW), and the strains' fatty acid composition is calculated as the percentage (%) of each chain length on the total amount of lipids. Displayed are the average (dot) and standard deviation (error bar) of at least three replicates.

Downloaded from https://academic.oup.com/jimb/article/50/1/kuad031/7281721 by guest on 07 November 2023

Overall, these results indicate that the gene deletions have a major effect on cell physiology and lipid chain composition under N-lim. On the other hand, under C-lim, cell physiology resulted mainly unchanged and we could only detect small changes in the FA chain length of the lipids. Since the Q4 strain showed altered lipid chain abundances compared to the wild-type strain, we performed a more detailed lipid analysis (solid-phase extraction [SPE]). We separated the different lipid classes to validate if differences were in membrane lipids, storage lipids, or free fatty acids (FFA).

Q4 Strain Shows Higher FFA and PL Fractions on N-lim

The FAME analysis only provides insight into the changes in the total lipid composition of the cell but does not discriminate between different lipid classes, such as neutral lipids (NL, consisting of DAGs, TAGs, and SE), FFA, and PL (mainly found in membranes). Therefore, we performed a SPE (Kaluzny et al., 1985), which separates the NL, FFA, and PL fractions and analyzes the FA distribution of each fraction.

Under C-lim, there are no statistically significant differences (p-value > 0.01) between the Q4 and the wild-type strain. Regardless of the strain, 73%–77% of the lipids are PL (Fig. 3), followed by 16%–23% of NL and 4%–7% of FFA. The chain length distribution of the PL fraction shows statistically significant differences (p-value < 0.01), but the entity of the change is less than 5% (Fig. 3). We detected no significant differences in the chain length distribution of NL (Fig. 3). In the FFA fraction, the Q4 strain has higher percentages of unsaturated lipids (C16:1, C18:1, and C18:2), while the saturated lipids (C16:0 and C18:0) are more abundant in the wild-type strain OKYL029 (Fig. 3). However, it is worth noting that the FFA fraction only contributes minorly to the overall lipid content (7% in the Q4 strain and 4% in the OKYL029 strain).

In the OKYL029 strain, the NL fraction accounts for only 23% of the total cell lipids in C-lim, compared to 60% in N-lim (Fig. 3), while the PL fraction decreased (from 73% to 36%). The FFA fraction only accounts for 4% of the total cell lipids in both C/N ratios in the OKYL029 strain. In the Q4 strain, the share of the NL fraction remained similar (15%–16%) in both C-lim and N-lim (Fig. 3). The PL fraction decreased 7% (77% in C-lim, 70% in N-lim), and the FFA fraction doubled (7% in C-lim to 15% in N-lim). In N-lim, regardless of the lipid fraction, C16:1 and C18:2 have a higher share in the Q4 strain than the wild-type strain. The C18:1 is more abundant in the wild type, regardless of the lipid class. The C18:0 is more abundant in the FFA and NL fractions of the OKYL029 strain, while the C16:0 only shows minor changes between strains.

These observations indicate that under C-lim, the Q4 strain only shows minor differences in the lipid fractions compared to the wild-type strain, confirming the results from our previous FAME analysis. On the other hand, under N-lim, the Q4 strain shows higher FFA and PL fractions. These results indicate that the deletions in TAG and SE synthesis mainly affect the cell phenotype when lipid synthesis is stimulated under N-lim.

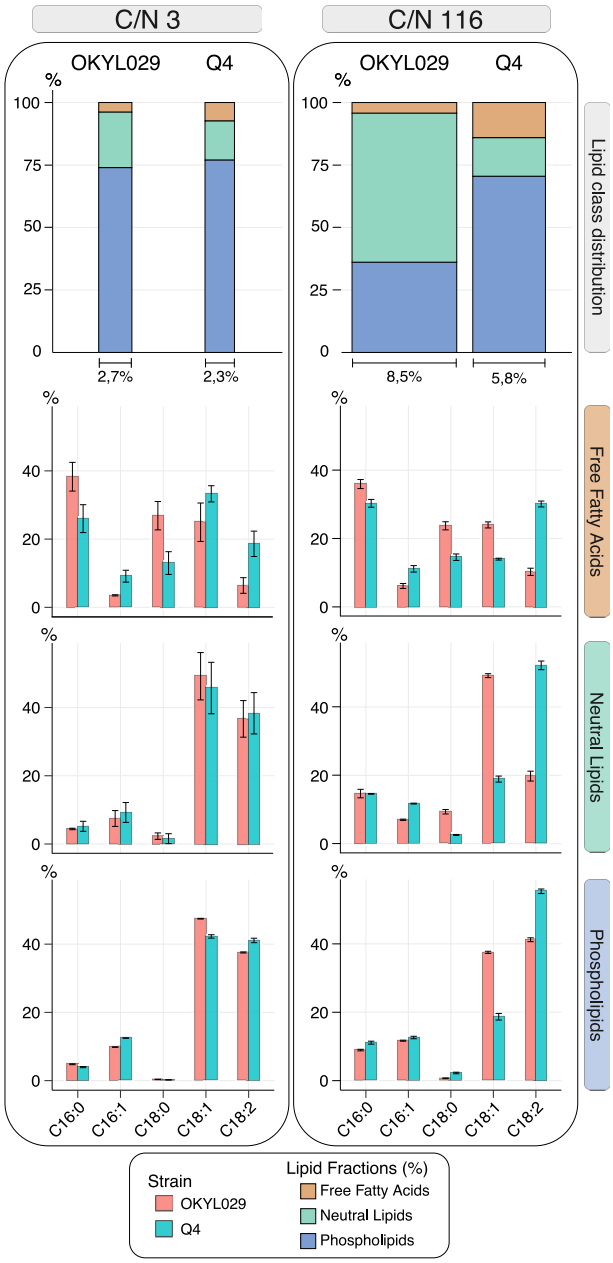

Fig. 3. Solid-phase extraction (SPE) of Q4 and OKYL029 in C-lim and N-lim conditions. Stacked bar charts (lipid class distribution) represent the share of each lipid class detected by SPE over the total amount of lipids present in the cell. The strains OKYL029 and Q4 were analyzed in C-lim and N-lim. The bar chart area is proportional to the total lipid content of the cell. The bottom three bar charts represent the fatty acid composition of each lipid fraction (free fatty acids, neutral lipids, and phospholipids), calculated as the percentage (%) of each chain length on the amount of lipids in that specific lipid class. Displayed are the average and standard deviation of at least three replicates.

FA Supplementation Affects the Growth of the Q4 Strain

Previous studies in *Saccharomyces cerevisiae* suggested a crucial interplay between lipid synthesis, LDs, and protein homeostasis (Olzmann & Carvalho, 2019). It has been reported that a storage lipid-free Q4 strain of *S. cerevisiae* (Δ*ARE1*, Δ*ARE2*, Δ*DGA1*, and Δ*LRO1*) shows higher sensibility toward unsaturated FA supplementation, indicating the important role TAGs have in FA buffering and detoxification (Petschnigg et al., 2009).

To assess the sensitivity of *Y. lipolytica* toward unsaturated FA, we calculated the molar concentrations of each FA (C16:0, C16:1, C18:0, C18:1, and C18:2) in the FFA fraction and in the total lipids of the OKYL029 and Q4 strains cultivated in C-lim and N-lim (Supplementary Fig. 4). The highest FA concentration calculated

Downloaded from https://academic.oup.com/jimb/article/50/1/kuad031/7281721 by guest on 07 November 2023

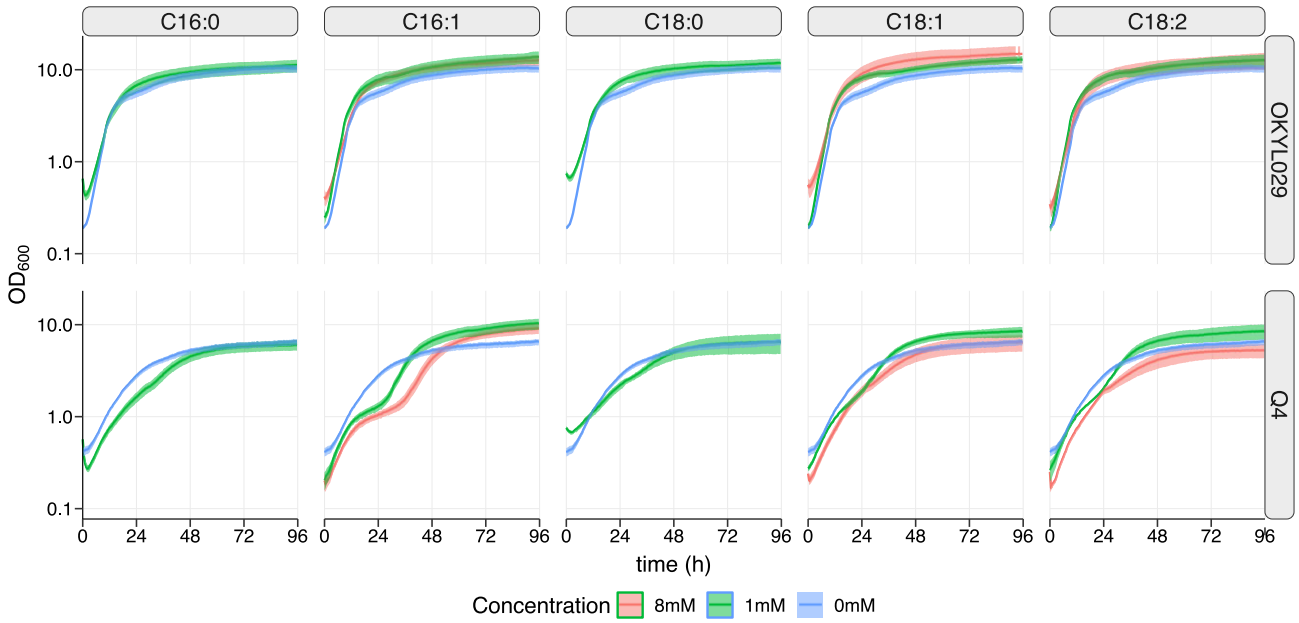

Fig. 4. Growth curves of *Y. lipolytica* strains Q4 and OKYL029 on delft media containing 2% ethanol and 1% Tween-20. The media was supplemented with different concentrations of fatty acid. Strains were cultured in 96-well plates and the OD_{600} was measured with the growth profiler every 30 min. The lines and shadows represent the average and standard deviation of five replicates.

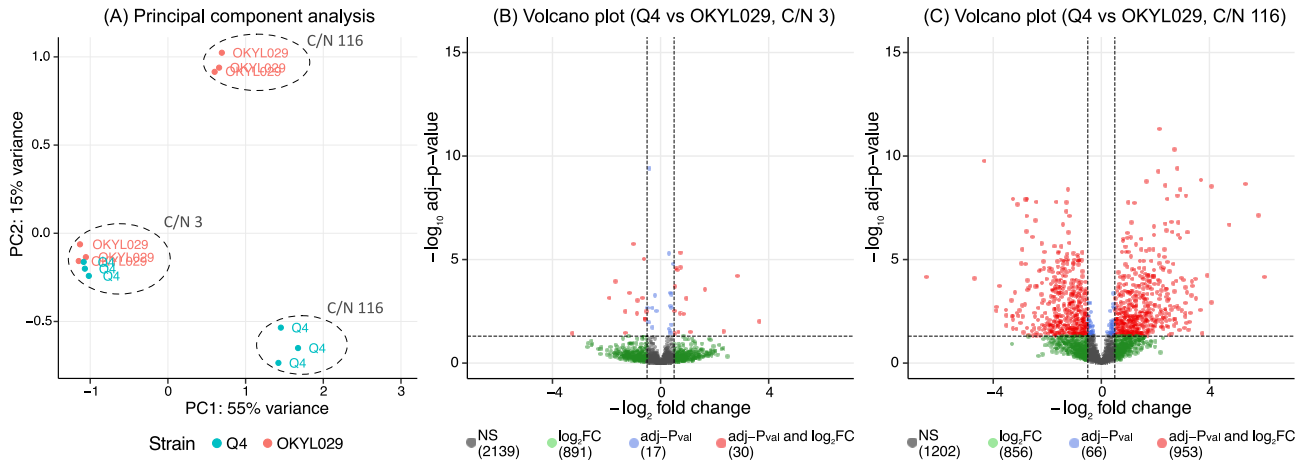

Fig. 5. RNA-sequencing of *Y. lipolytica* strains Q4 and OKYL029 in carbon (C/N ratio 3) and nitrogen (C/N ratio 116) limitation. (A) principal component analysis. Volcano plots for samples in carbon (B) and nitrogen limitation (C). NS: non-significative genes. Log_2FC: genes with an absolute fold change greater than 0.5. Adj-*p*-value: genes with an adjusted *p*-value below 0.05. Log_2FC and adj-*p*-val: genes with both adjusted *p*-value below 0.05 and absolute log_2 fold change greater than 0.5.

in the FFA fraction is 7 μm (C16:0). When considering the total lipids, the highest concentration measured is 1.5 mM (C18:1). We tested these concentrations, but no effect was visible (data not shown). Therefore, we decided to test the highest concentrations that solubility allowed in our experimental setup, and supplemented cultivations with up to 8 mM of unsaturated FA and up to 1 mM of saturated FA (Fig. 4).

Overall, the Q4 strain is more sensitive to FA, while the wild-type strain was unaffected even by high concentrations. For example, supplementation of the unsaturated palmitoleic acid (C16:1) did not affect OKYL029, while it induced a different growth profile in the Q4 strain. The Q4 strain exhibited two exponential growth phases that were interrupted by a period of reduced growth. Even though FFA affects the growth of the Q4 strain, the strain is less sensitive to FA supplementation compared to *S. cerevisiae*, in which concentrations above 0.5 mM delay or inhibit growth (Garbarino et al., 2009).

Gene Deletions Affect Gene Expression in N-lim but Not in C-lim

To elucidate how the four deletions impact cell regulation, we performed transcriptomic analysis (RNA-sequencing [RNA-seq]) on pH-controlled chemostat samples from the Q4 and OKYL029 strains, in C-lim and N-lim.

Similarities and dissimilarities between samples were assessed with principal component analysis (PCA) (Fig. 5A). The first two principal components, respectively, account for 55% and 15% of the total variance of the RNA-seq dataset. The PCA shows that the two main experimental factors, C/N ratio and strain background,

Downloaded from https://academic.oup.com/jimb/article/50/1/kuad031/7281721 by guest on 07 November 2023

separate the samples and account for most of the variability. Additionally, samples in C-lim cluster together, regardless of their genetic background, while samples are separated by genetic background in N-lim when lipid accumulation is stimulated. These results align well with both phenotype and lipid measurements, where in C-lim both strains are very similar, while in N-lim the strains show major differences.

To identify changes in expression levels and to identify which genes are differentially expressed between samples, we performed differential gene expression analysis and compared the Q4 strain with the OKYL029 in C-lim and N-lim. As expected, after *p*-value adjustment, for samples clustered together in C-lim, we only detected 30 differentially expressed genes, either upregulated or downregulated (absolute $\log_2$ fold change greater than 0.5 and adjusted *p*-value below 0.05) (Fig. 5B). For each differentially expressed gene, we checked the annotated function on UniProt. Unfortunately, most of these genes have an unknown function, and we only found six genes associated with a protein function (Supplementary Table 1). Three of these genes are related to lipid metabolism ("triacylglycerol lipase", "glycerophosphocholine phosphodiesterase", and "glycolipid 2-α-mannosyltransferase-domain-containing protein") and might contribute to the small differences we observed in lipid composition between strains in carbon limiting conditions.

The major difference between strains is in N-lim, where nitrogen depletion triggers lipid accumulation. As expected from the PCA results, we see major differences between strains. By comparing the Q4 strain to OKYL029, we found a total of 953 differentially expressed genes (absolute $\log_2$ fold change above 0.5 and adjusted *p*-value below 0.05) (Fig. 5C). Out of the total 953 differentially expressed genes, 390 have a function annotated on UniProt (Supplementary Table 2).

In summary, the low variance identified in the PCA, and the low number of genes differentially expressed indicate that the deletions have minimal effect on the overall transcriptome in C-lim. On the other hand, the variance identified in the PCA and the high number of differentially expressed genes indicate a major effect of the deletions in N-lim.

Gene Set Analysis Reveals Upregulation of Misfolded Protein Gene Sets

The high number of differentially expressed genes in the Q4 strain under N-lim hinders single-gene analysis. To draw biological conclusions, we performed a gene set analysis (GSA). In a GSA, gene sets are defined based on prior biological knowledge to determine whether a defined gene set shows statistically significant differences between samples (Maleki et al., 2020). Gene sets can be defined using gene ontology (GO) terms (Ashburner et al., 2000). GO terms are generally divided into biological process, molecular function, and cellular component. For each of these levels, we performed a GSA with the R package PIANO (Väremo et al., 2013), using gene-level statistics calculated with TMM-normalized gene counts (Fig. 6).

A biological process represents a specific objective that the organism is genetically programmed to achieve, for example, the biological process of cell division, and is carried out by specific gene products in a regulated manner (Thomas, 2017). In the biological process, we found 12 GO terms that are significantly enriched in the Q4 strain. Among them, broad GO terms such as "protein folding", "protein refolding", and "cellular response to unfolded protein" are enriched. Two GO terms related to chaperones and chaperones activity are enriched in the Q4 strain, namely, "chaperone-mediated protein complex assembly" and

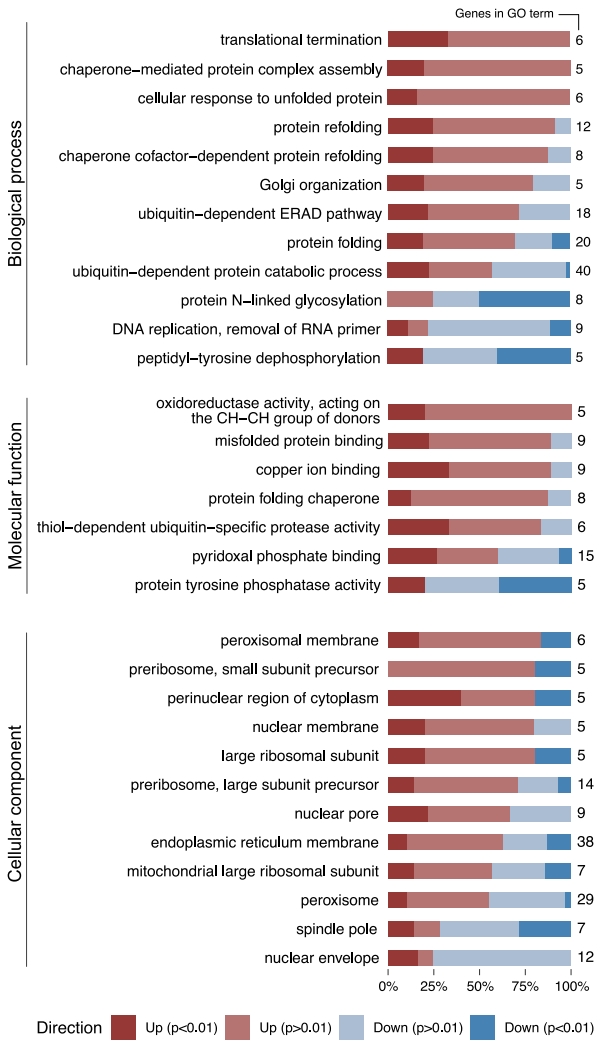

Fig. 6. Gene set analysis (GSA) of Q4 versus OKYL029 in N-lim (C/N ratio 116). Gene sets are defined by GO terms (biological process, molecular function, and cellular component). For each gene set that is significantly enriched, the direction of the relative changes in RNA levels (positive or negative fold change) is shown, and the genes in the gene sets are marked based on significative or non-significative adjusted *p*-value (cut-off 0.05). Genes are considered up or down in the Q4 strain, and the OKYL029 strain is the reference strain. The total number of genes in each gene set is reported on the right.

"chaperone cofactor-dependent protein refolding". Chaperones are proteins that assist in the conformational folding of proteins during or after synthesis, and after partial denaturation (Buchner, 2019). An enrichment of chaperone-related processes indicates that the cell has activated mechanisms to handle folding stress. We also found that ubiquitin-related GO terms are enriched. The "ubiquitin-dependent ERAD pathway" targets ER-resident proteins for degradation to the cytoplasmic proteasome (Thibault & Ng, 2012). The "ubiquitin-dependent protein catabolic process" is a group of reactions resulting in protein degradation, and is initiated by multiple ubiquitin groups binding to the protein targeted for degradation (Finley et al., 2012). Two other GO terms ("Golgi organization" and "protein N-linked glycosylation") are enriched in the Q4 strain and can be linked to unfolded protein response (UPR). Most genes in the GO term "Golgi organization" are upregulated. Signaling to transcribe genes for Golgi organization is active, suggesting that a proper Golgi organization is missing. The genes in the "protein N-linked glycosylation" are mainly downregulated,

Downloaded from https://academic.oup.com/jimb/article/50/1/kuad031/7281721 by guest on 07 November 2023

suggesting that transcription of genes responsible for glycosylation is not required. This can be due to newly synthesized proteins being misfolded and targeted for degradation instead of being transported to the Golgi apparatus for glycosylation. Two GO terms ("translation termination" and "DNA replication removal of RNA primer") are related to cell growth and replication. For the GO term "peptidyl-tyrosine dephosphorylation", the annotation is insufficient to reconstruct its precise biological significance, but dephosphorylation and phosphorylation of tyrosine residues modulate the enzymatic activity and creates, binding sites for the recruitment of downstream signaling proteins (Hunter, 1995).

A molecular function term describes activities that occur at the molecular level and are carried out by individual gene products or by molecular complexes composed of multiple gene products (Thomas, 2017). In the molecular function, we found seven significantly enriched GO terms in the Q4 strain. Three GO terms ("misfolded protein binding", "protein folding chaperone", and "thiol-dependent ubiquitin-specific protease activity") are broadly related to misfolded protein response. Two GO terms ("copper ion binding" and "oxidoreductase activity, acting on the CH-CH group of donors") play important roles in many biochemical processes such as oxidation, dioxygen transport, and electron transfers. The lack of further annotation prevents the reconstruction of more detailed molecular functions for these gene sets. "Pyridoxal phosphate binding" is related to pyridoxal phosphate, the active form of the B6 vitamin, that acts as a cofactor for enzymes involved in the biosynthesis of amino acids and amino acid-derived metabolites (Hayashi, 1995). "Protein tyrosine phosphorylation" is a post-translational modification that creates novel recognition motifs for protein interactions and cellular localization (Hunter, 1995).

Cellular component is the location occupied by a macromolecular machine when it carries out a molecular function (Thomas, 2017). It can be relative to cellular compartments, structures, or macromolecular complexes (e.g., the ribosome). We found 12 differentially enriched GO terms in the Q4 strain that are mainly related to transcription and translation. Four GO terms related to the nucleus ("perinuclear region of cytoplasm", "nuclear membrane", "nuclear pore", and "nuclear envelope"), three GO terms related to the ribosomes ("preribosome, small subunit precursor", "large ribosomal subunit", and "preribosome, large subunit precursor"), and one GO term related to the "endoplasmid reticulum membrane" are enriched in the Q4 strain. Since LD originates within the ER membrane and their formation is specially coordinated by nuclear-vacuolar junctions (Graef, 2018; Hariri et al., 2018), suppressing LD formation in the Q4 strain (Supplementary Fig. 3) could affect the nuclear, ribosomial, and ER organization. Additionally, we saw an enrichment of two GO terms related to the peroxisomes ("peroxisomal membrane" and "peroxisome"), and the GO terms "mitochondrial large ribosomal subunit", and "spindle pole".

Our results show that many GO terms related to UPR, chaperones, and ubiquitin are enriched in the Q4 strain. Molecular functions and cellular components related to UPR response are also affected, indicating that the cell is experiencing folding stress, and protein synthesis and functionality are affected by the four deletions. These results suggest a link between physiological lipid production and protein homeostasis.

Discussion

Deleting lipid genes has proven a valid strategy to boost added value and commodity chemical production in *Y. lipolytica* (Shi et al., 2021; Fu et al., 2023), but it would be undesired if those deletions would negatively impact cell physiology and reduce cell resilience and robustness. In this context, our goal was to elucidate the consequences of deleting four genes involved in lipid metabolism (*DGA1*, *DGA2*, *ARE1*, and *LRO1*). We cultivated the Q4 strain (JFYL007) carrying the four deletions and the wild-type strain (OKYL029) either in carbon or nitrogen-limiting conditions and performed RNA-seq. We showed that in C-lim, physiological parameters and the transcriptome only show a few minor changes, while in N-lim, when the carbon flux toward lipid synthesis is high, cell physiology and the transcriptome are strongly affected by the deletions. Furthermore, we show that in N-lim, the lipid organization of the Q4 strain is altered, and multiple GO terms related to UPR are enriched in the transcriptome.

In N-lim, the SPE analysis revealed that the lipid distribution in NL, PL, and FFA is affected in the Q4 strain. While the wild-type strain showed a predominant NL fraction, the Q4 strain has reduced amounts of NL, and PL are predominant. The FFA fraction in the Q4 strain is 3 times larger than in the wild-type strain, indicating that the Q4 strain is synthesizing FFA but lacks the ability to incorporate it into TAGs. Lipid homeostasis is maintained by balancing NL synthesis and lipid turnover (Koch et al., 2014). To avoid possible toxic and membrane-disturbing effects, FFA are stored as NL, which are biologically inert (Koch et al., 2014). In *Y. lipolytica*, the NL fraction mainly contains TAGs, and only small amounts of SE (Beopoulos et al., 2012). The Q4 strain lacks four genes responsible for TAG and SE synthesis. In C-lim, lipid synthesis is not stimulated, and the genotypical difference between the Q4 strain and the wild-type strain is not visible in the phenotype. In N-lim, the flux through the four enzymes of the lipid accumulation pathway is high (Beopoulos et al., 2008; Kerkhoven et al., 2016), and their absence prevents FFA from being incorporated into TAGs.

A storage lipid-free Q4 strain of *S. cerevisiae* (Δ*ARE1*, Δ*ARE2*, Δ*DGA1*, and Δ*LRO1*) shows high sensibility toward FFA supplementation, suggesting the important role TAGs play in FA buffering and detoxification (Petschnigg et al., 2009). FFA could act as detergents, interfering with membrane integrity, or could be incorporated into lipid species that are cytotoxic at high levels, such as ceramide, acylcarnitine, and DGA (Olzmann & Carvalho, 2019). In wild-type strains, to prevent lipotoxicity, excess FFA are incorporated into TAGs, which are in turn stored in LDs (Koch et al., 2014; Friedlander et al., 2016). The Q4 strain of *Y. lipolytica* cannot synthesize LDs (Gajdoš et al., 2016) (Supplementary Fig. 3). The higher levels of FFA detected in the Q4 strain under N-lim, and their reported cytotoxicity may be the reason for the lower CDW reached by the Q4 strain during the fermentation, which was 33% lower compared to the wild-type strain. We investigated *Y. lipolytica's* sensitivity toward FA (Fig. 4) and showed that the Q4 strain is more sensitive to high concentrations of unsaturated FA than the wild-type strain. The growth of the Q4 strain was affected by FFA, but the strain was able to grow in media supplemented with 8 mM FFA. The Q4 strain of *Y. lipolytica* is less sensitive to FA supplementation than the Q4 strain of *S. cerevisiae*, in which concentrations of 0.5 mM delay or inhibit growth (Garbarino et al., 2009). Additionally, if a downstream pathway is integrated into the Q4 strain, the acyl-CoA flux would be redirected to other products, which should prevent the accumulation of FFA.

RNA-seq and GSA revealed an enrichment of multiple GO terms connected to the UPR when the Q4 strain was cultivated under N-lim conditions. We found broad GO terms contributing to the UPR response and four GO terms related to chaperones and ubiquitin-dependent activities enriched in the Q4 strain. Chaperones are

Downloaded from https://academic.oup.com/jimb/article/50/1/kuad031/7281721 by guest on 07 November 2023

proteins that assist the conformational folding of proteins during or after synthesis, and after partial denaturation (Buchner, 2019). Ubiquitin-dependent activities are responsible for targeting proteins for degradation (Finley et al., 2012; Thibault & Ng, 2012). The Q4 strain shows enrichment of chaperone and ubiquitin-related GO terms, indicating that the cells are experiencing folding stress. The enrichment of Golgi-related GO terms further supports this observation. Proteins are glycosylated in the Golgi apparatus before being targeted for delivery to their final destination (Suda & Nakano, 2012). The genes in the "protein N-linked glycosylation" GO term are mainly downregulated, suggesting that newly synthesized proteins might be misfolded and targeted for degradation before being transported to the Golgi apparatus for glycosylation. The genes of the "Golgi organization" GO term are mainly upregulated, suggesting that a proper Golgi organization might be lacking. Taken together, these results suggest that a major alteration in lipid metabolism affects protein synthesis and functionality.

The Q4 strain lacks the ability to synthesize LDs (Gajdoš et al., 2016) (Supplementary Fig. 3) and displays alterations in the quantity and lipid distribution, activation of the UPR response, and enrichment of several GO terms related to proteostasis. These observations indicate that cell homeostasis is linked with LD biology and functionality, as was previously shown in *S. cerevisiae* (Graef, 2018). Lipids are synthesized and aggregated on the ER membrane, where they form LD that can bud from the ER membrane (Jacquier et al., 2011). LDs have an NL core surrounded by a monolayer of PL, usually associated with proteins (Jacquier et al., 2011). LDs have been shown not only to act as lipid storage but also to prevent lipotoxicity by buffering FA stress (Petschnigg et al., 2009; Nguyen et al., 2017) and to have an active role in membrane and organelle homeostasis (Petschnigg et al., 2009; Velázquez et al., 2016; Graef, 2018). LDs are important in starvation-induced autophagy (Deretic, 2015; Velázquez et al., 2016), clearance of inclusion bodies (Moldavski et al., 2015), and, ultimately, in proteostasis (Moldavski et al., 2015; Velázquez et al., 2016). Starvation-induced autophagy, for example, during nitrogen starvation, is a physiological process involved in protein and organelle degradation in the lysosomes (Deretic, 2015); inclusion bodies are non-toxic and non-soluble aggregates of misfolded proteins. LDs participate in starvation-induced autophagy and physically associate with inclusion bodies, contributing to their degradation (Moldavski et al., 2015). Proteostasis is the group of processes that regulate protein synthesis and degradation within the cell. LDs are involved in proteostasis mechanisms and have an important role in contributing to stress resistance, cell survival, and, ultimately, cell homeostasis. Deleting gene involved in lipid metabolism in *Y. lipolytica* results in cells that lack LDs, which are important organelles in cell homeostasis. This results in cells with altered lipid composition and proteome, and with upregulation of the UPR response.

To summarize, our work reveals the connection between lipid metabolism, protein regulation and folding, and cell homeostasis. Deleting the genes *DGA1*, *DGA2*, *LRO1*, and *ARE1* blocks TAG and SE accumulation in the Q4 strain, and results in the absence of LDs. LDs play an important role in lipid homeostasis and participate in the clearance of misfolded proteins and inclusion bodies. Lacking LDs, the Q4 strain not only shows altered lipid class distribution, but also an abundance of potentially cytotoxic FFA, and an enrichment of GO terms related to the UPR response, protein degradation, and Golgi activities. Our findings highlight the importance of lipid metabolism in *Y. lipolytica* and the implications of abolishing TAG synthesis on cell physiology and proteostasis. Our findings can aid in the development of improved chassy strains of *Y. lipolytica* for commodity chemical production, where lipid synthesis is not abolished but downregulated to maintain cell robustness and physiological activities.

Mateirals and Methods

Yeast Strains

The strains used in the study are derived from the *Y. lipolytica* strain ST6512 (Marella et al., 2020), which was derived from the W29 background strain (Y-63746 from the ARS Culture Collection, Peoria, IL, USA) (also known as ATCC20460/CBS7504). ST6512 has been engineered to harbor a KU70::Cas9-DsdA system, which allows for marker-free genomic engineering using the EasyCloneYALI toolbox (Holkenbrink et al., 2018). The strain OKYL029 (ST6512 Δmhy1) has a deletion of the MHY1 gene to prevent stress-induced hyphae formation (Konzock & Norbeck, 2020). The strain OKYL049 (ST6512 + E1::pTef1in + DGA1 + tPEX20 Δare1 Δmhy1) is an obese strain that carries overexpression of the DGA1 gene and a deletion of the ARE1 gene to increase TAG accumulation and abolish SE formation (Konzock et al., 2021). To prevent hyphae formation, the MHY1 gene is also deleted in this strain. The Q4 strain JFYL007 (ST6512 Δmhy1 Δare1 Δlro1 Δdga1 Δdga2) is a low-lipid-accumulating strain that carries deletions of the ARE1, LRO1, DGA1, and DGA2 genes to decrease TAG accumulation, and a deletion of the MHY1 gene to prevent hyphae formation (Poorinmohammad et al., 2022). The gene annotation for these strains follows the YALI1 system, but translation into YALI0/CLIB122 can be done with the Supplementary Table 2 of Magnan et al. (2016).

Shake Flask Cultivation

To select suitable C/N ratios for chemostat cultivations, *Y. lipolytica* was grown for 5 days in delft media containing 7.5 g/L ammonium sulphate (Sigma-Aldrich, 7783-20-2), 14.4 g/L magnesium sulphate heptahydrate (Merck, 10034-99-8), 0.5 g/L potassium dihydrogen phosphate (Sigma-Aldrich, 7778-77-0), 1 mL of trace metals solution, and 1 mL of vitamin solution. The pH of the media was set at 5.0 by potassium hydroxide (Avantor, VWR, 1310-58-3) addition. The glucose (Avantor, VWR, 14431-43-7) concentration was varied between 3 g/L and 60 g/L to obtain C/N ratios between 1 and 20.

Trace metal solution consisted of 3 g/L iron(II) sulfate heptahydrate ($FeSO_4 7\ H_2O$) (Sigma-Aldrich, 7782-63-0), 4.5 g/L zinc sulfate heptahydrate ($ZnSO_4 7\ H_2O$) (Sigma-Aldrich, 7446-20-0), 4.5 g/L calcium chloride dihydrate ($CaCl_2 2\ H_2O$) (Sigma-Aldrich, 10035-04-8), 1.0 g/L manganese(II) chloride tetrahydrate ($MnCl_2 4\ H_2O$) (Sigma-Aldrich, 13446-34-9), 300 mg/L cobalt(II) chloride hexahydrate ($CoCl_2 6\ H_2O$) (Sigma-Aldrich, 7791-13-1), 300 mg/L copper(II) sulfate pentahydrate ($CuSO_4 5\ H_2O$) (Sigma-Aldrich, 7758-99-8), 400 mg/L sodium molybdate dihydrate ($Na_2MoO4 2\ H_2O$) (Sigma-Aldrich, 10102-40-6), 1.0 g/L boric acid (H_3BO_3) (Sigma-Aldrich, 10043-35-3), 100 mg/L potassium iodide (KI) (Sigma-Aldrich, 7681-11-0), and 19 g/L disodium ethylenediaminetetraacetate dihydrate ($Na_2EDTA2\ H_2O$) (Sigma-Aldrich, 6381-92-6). Vitamin solution consisted of 50 mg/L D-biotin (Sigma-Aldrich, 58-85-5), 1.0 g/L D-pantothenic acid hemicalcium salt (Sigma-Aldrich, 137-08-6), 1.0 g/L thiamin HCl (Sigma-Aldrich, 67-03-8), 1.0 g/L pyridoxin HCl (Sigma-Aldrich, 58-56-0), 1.0 g/L nicotinic acid (Sigma-Aldrich, 59-67-6), 0.2 g/L 4-aminobenzoic acid (Sigma-Aldrich, 150-13-0), 25 g/L myo-inositol (Sigma-Aldrich, 87-89-8).

Downloaded from https://academic.oup.com/jimb/article/50/1/kuad031/7281721 by guest on 07 November 2023

Growth Profiler

To investigate FA toxicity, *Y. lipolytica* strains OKYL029 and JFYL007 (Q4) were cultivated in 96-well plates at 30°C and 200 rpm. Growth performances were determined with Growth Profiler 960 (EnzyScreen BV, Heemstede, The Netherlands) using a standard sandwich cover with pins (CR1396b) with OD_{600} measurement every 30 min. To determine the growth performances, cells were grown in 150 μL of delft media (N-lim, C/N 116) containing 1% Tween-20, 2% ethanol, and FA (C16:0, C16:1, C18:0, C18:1, and C18:2) at a final concentration of 8 or 1 mM. The controls were grown in 150 μL of delft media (N-lim, C/N 116) containing 1% Tween-20 and 2% ethanol. The starting OD_{600} for cell cultivation was 0.1. Each experiment was carried out in quintuplicate. Growth curves represent the average of quintuplicates, and error bars are represented as shadowed areas.

Bioreactor and Chemostat Cultivation

Chemostat cultivations were performed as described in Konzock et al. (2022). Cultivations were carried out in DASGIP 1-L stirrer-pro vessels (Eppendorf, Jülich, Germany). The working volume was 500 mL, the temperature was kept at 28°C, and the agitation was set at 600 rpm. To ensure aerobic conditions, sterile airflow was set at 1 vvm (= 30 L hr^{-1}) and dissolved oxygen was monitored with DO probes (Mettler Toledo, Switzerland). The pH was monitored with a pH sensor (Mettler Toledo, Switzerland) and maintained at 5.0 ± 0.05 by automatic addition of 2 M KOH. Batch cultivations were performed with the same media as chemostat cultivations, and cell growth was monitored via the CO_2 exhaust gas. After the cells left the exponential growth phase, the constant feed was initiated to obtain steady-state cultivation with a dilution rate of 0.10 hr^{-1} for OKYL029 and Q4 strains. The working volume of 500 mL was maintained using an overflow pump. Samples for transcriptome analysis were taken after at least 4 residence times of steady-state growth, and each condition was cultivated at least in triplicates.

Chemostat cultivations with C/N ratio 3 (C-lim) were performed in delft media containing 5.28 g/L of ammonium sulphate, 7.92 g/L glucose, 0.5 g/L magnesium sulphate heptahydrate, 3 g/L monopotassium phosphate, 1 mL of trace metals solution, and 1 mL of vitamin solution. Trace metal and vitamin solutions have the same composition as in shake flask cultivations.

The pH was set at 5 with 2 M KOH and was kept at 5 during the fermentation by automatic KOH addition.

Chemostat cultivations with a C/N ratio 116 (N-lim) were performed in delft media containing 0.471 g/L of ammonium sulphate, 27.5 g/L glucose, 0.5 g/L magnesium sulphate heptahydrate, 3 g/L monopotassium phosphate, 1 mL of trace metal solution, and 1 mL of vitamin solution. Trace metal and vitamin solutions have the same composition as in shake flask cultivations. The pH was set at 5 with 2 M KOH and was kept at 5 during the fermentation by automatic KOH addition.

Extracellular Metabolite Analysis

Samples for high-performance liquid chromatography (HPLC) were taken after at least four residence times of steady-state cultivation. A volume of 1 mL of culture was centrifuged (5 min, 3000 rcf), and the supernatant was used for HPLC analysis. Acetate, citrate, ethanol, glycerol, glucose, pyruvate, and succinate concentrations were quantified. The HPLC system UltiMate® 3000 (Dionex, Sunnyvale, CA, USA) was equipped with an Aminex® HPX-87H ion exclusion column (Bio-Rad, Hercules, CA, USA). 5 mM H_2SO_4 at a flow rate of 0.6 mL/min was used as an eluent. Glucose was quantified using a refractive index detector (Shodex RI-101).

Lipid Extraction and Quantification

Samples for lipid extraction and quantification were taken after at least four residence times of steady-state cultivation. The protocol used was previously described (Qiao et al., 2015; Konzock & Norbeck, 2020). Briefly, 1 mL of cell culture was spun down (5 min, 5000 rcf), the supernatant discarded, and the pellet washed twice with 1 mL water. The resuspended cells were spun down (5 min, 5000 rcf), and the pellet was resuspended in 100 μL of water. The suspension was dried in a vacuum-dried freezer for 1 day. A total volume of 40 μg of triheptadecanoin [TAG(17:0/17:0/17:0)] were then added to the freeze-dried cell pellet as an internal standard. After adding 500 μL of 1 M NaOH in methanol, the samples were vortexed at 1200 rpm for 1 hr (room temperature). After adding 80 μL of 49% sulfuric acid, FAMEs were extracted by adding 500 μL of hexane. Phases were separated by centrifugation (1 min, 10 000 rcf), and 200 μL of the upper hexane phase were diluted 1:5 in hexane. A volume of 1 μL was analyzed on GC-MS (Thermo Scientific Trace 1310 coupled to a Thermo Scientific ISQ LT with a ZBFAME column [Phenomenex, length: 20 m; inner diameter: 0.18 mm; film thickness: 0.15 μm]). The method consisted of 2 min hold at 80°C, followed by a ramp of 40°C/min until 160°C, a ramp of 5°C/min until 185°C, a ramp of 40°C/min until 260°C, and a final hold of 260°C for 30 s.

Lipid content was calculated as lipid content percentage over the CDW. CDW was determined by vacuum filtration of 1 mL of samples on pre-weighed 0.45 µm filter membranes (Sartorius Biolab), followed by 15 min microwaving at 325 W and placement in a desiccator for at least 3 days.

Solid-Phase Extraction

Samples for SPE were taken after at least four residence times of steady-state cultivation. The protocol has been adapted from Kaluzny et al. (1985). Briefly, after adding 1 mL of chloroform:methanol 2:1 (v:v) (Merck), the sample was vortexed at 1200 rpm for 1 hr at room temperature. SPE cartridges (Supelclean™ LC-NH2 SPE Tube; Sigma-Aldrich) were placed on Vac Elut apparatus and activated with 4 mL of hexane. Samples were then loaded on the cartridges and eluation of the different lipid fractions was achieved by adding solvents in the following order. To elute the NL fraction, 4 mL of chloroform:isopropanol 2:1 (v:v) (Merck) were used, including cholesterol, cholesterol ester, triacylglycerol (TAG), diacylglycerol (DAG), and monoacylglycerol (MAG). To elute the FFA fraction, 4 mL of 2% acetic acid in diethyl ether (Sigma-Aldrich) were used. To elute the PL fraction, 4 mL of methanol were used. The lipid fractions were collected, and the solvent was evaporated in a MiVac apparatus (35°C, 1 hr). Pellets were then resuspended in 1 mL chloroform:methanol 2:1 (v:v), transferred to 1.5 mL reaction tubes, and subjected to FAME extraction before analysis on GC-MS. For SPE samples, the GLC reference standard GLC 426 was used, and the method consisted of 2 min hold at 80°C, followed by a ramp of 40°C/min until 120°C, a ramp of 3.5°C/min until 165°C, a ramp of 40°C/min until 260°C, and a final hold of 260°C for 30 s.

RNA Extraction and Sequencing

Samples for RNA extraction were taken after at least four residence times of steady-state cultivation. A total volume of 10 mL of culture were rapidly withdrawn and injected into a 50 mL falcon tube containing ca. 35 mL of crushed ice. Samples were immediately centrifuged (5 min, 4000 rcf, 4°C). After discarding the supernatant, the pellet was resuspended in 2 mL ice-cold water, transferred into 2 mL reaction tubes, and centrifuged (5 min, 4000 rcf, 4°C). The supernatant was discarded, and to remove the

Downloaded from https://academic.oup.com/jimb/article/50/1/kuad031/7281721 by guest on 07 November 2023

remaining supernatant residues, reaction tubes were tapped on paper towels. Samples were immediately frozen in liquid nitrogen and stored at −80°C until RNA extraction.

RNA was extracted using the RNeasy Mini Kit (QIAGEN, Hilden, Germany). DNA present in the samples was digested using RNase-Free DNase Set (QIAGEN). The quality of RNA samples was analyzed with a 2100 Bioanalyzer (Agilent Technologies, Inc., Santa Clara, CA, USA). The purified RNA was stored at −80°C until further analysis.

The RNA library was constructed using Illumina TruSeq Stranded mRNA (poly-A selection), and samples were sequenced on NovaSeq6000 (NovaSeq Control Software 1.7.5/RTA v3.4.4) with a 151nt(Read1)-10nt(Index1)-10nt(Index2)-151nt(Read2) setup using "NovaSeqXp" workflow in "S4" mode flowcell. The Bcl to FastQ conversion was performed using bcl2fastq_v2.20.0.422 from the CASAVA software suite. The quality scale used was Sanger/phred33/Illumina 1.8+. The raw data can be retrieved from ArrayExpress with access number E-MTAB-11008.

Differential Gene Expression and GSA

The raw reads were processed with the NGI RNAseq Pipeline (https://github.com/nf-core/rnaseq.git), version 3.5. The *Y. lipolytica* strain CLIB89(W29) reference genome was used to map the reads (assembly GCA_001761485.1). Differential gene expression analysis was performed with voom–limma (Law et al., 2014; Ritchie et al., 2015), and adjusted *p*-values were adjusted according to the Benjamini–Hochberg method. Volcano plots were made with the R package EnhancedVolcano (Kevin et al., 2022). OmicsBox (https://www.biobam.com/omicsbox) was used to generate gene sets by blasting *Y. lipolytica* exons against the RefSeq non-redundant proteins database using the BlastX algorithm. A total of 31.421 GO terms were annotated for 5629 genes. GSA was performed using the R package PIANO (Platform for Integrative Analysis of Omics) (Väremo et al., 2013), using gene level statistics, and excluding gene sets containing less than five or more than 500 genes. The code used for the analysis is available on GitHub (https://github.com/SysBioChalmers/Yarrowia_Multifactor).

Acknowledgments

The authors acknowledge support from the National Genomics Infrastructure in Stockholm funded by Science for Life Laboratory, the Knut and Alice Wallenberg Foundation and the Swedish Research Council, and the SNIC/Uppsala Multidisciplinary Center for Advanced Computational Science for assistance with massively parallel sequencing and access to the UPPMAX computational infrastructure.

The computations were enabled by resources provided by the Swedish National Infrastructure for Computing (SNIC) at Chalmers Centre for Computational Science and Engineering (C3SE), partially funded by the Swedish Research Council through grant agreement no. 2018-05973.

Supplementary material

Supplementary material is available online at *JIMB* (*www.academic.oup.com/jimb*).

Author contributions

S.Z. and O.K. contributed equally to the work. Conceptualization, S.Z., O.K., and E.J.K.; Methodology, S.Z., O.K., and J.F.; Formal Analysis, S.Z.; Investigation, S.Z.; Data Curation, S.Z.; Writing – Original Draft, S.Z.; Writing – Review & Editing, S.Z., O.K., and E.J.K.; Visualization, S.Z.; Funding Acquisition, E.J.K.

Funding

This research was funded by the Novo Nordisk Foundation (grant NNF20CC0035580), the Research Council for Environment, Agricultural Sciences, and Spatial Planning (Formas) (grant 2018-00597), the Swedish Research Council (VR) (grant 2019-04624), and Åforsk Foundation (grant 23-587).

Conflict of interest

The authors have no competing interests.

Data availability

The raw RNA-seq data are deposited in ArrayExpress with accession number E-MTAB-11008.

The code and data used for the analysis are deposited on GitHub and are available at https://github.com/SysBioChalmers/Yarrowia_Multifactor.

References

Ashburner, M., Ball, C. A., Blake, J. A., Botstein, D., Butler, H., Cherry, J. M., Davis, A. P., Dolinski, K., Dwight, S. S., Eppig, J. T., Harris, M. A., Hill, D. P., Issel-Tarver, L., Kasarskis, A., Lewis, S., Matese, J. C., Richardson, J. E., Ringwald, M., Rubin, G. M., . . . Sherlock, G. (2000). Gene ontology: Tool for the unification of biology. *Nature Genetics*, 25(1), 25–29. https://doi.org/10.1038/75556

Athenstaedt, K. (2011). YALI0E32769g (DGA1) and YALI0E16797g (LRO1) encode major triacylglycerol synthases of the oleaginous yeast *Yarrowia lipolytica*. *Biochimica et Biophysica Acta (BBA)—Molecular and Cell Biology of Lipids*, 1811(10), 587–596. https://doi.org/10.1016/j.bbalip.2011.07.004

Beopoulos, A., Haddouche, R., Kabran, P., Dulermo, T., Chardot, T., & Nicaud, J. M. (2012). Identification and characterization of DGA2, an acyltransferase of the DGAT1 acyl-CoA:Diacylglycerol acyltransferase family in the oleaginous yeast *Yarrowia lipolytica*. New insights into the storage lipid metabolism of oleaginous yeasts. *Applied Microbiology and Biotechnology*, 93(4), 1523–1537. https://doi.org/10.1007/s00253-011-3506-x

Beopoulos, A., Mrozova, Z., Thevenieau, F., Le Dall, M. T., Hapala, I., Papanikolaou, S., Chardot, T., & Nicaud, J. M. (2008). Control of lipid accumulation in the yeast *Yarrowia lipolytica*. *Applied and Environmental Microbiology*, 74(24), 7779–7789. https://doi.org/10.1128/AEM.01412-08

Buchner, J. (2019). Molecular chaperones and protein quality control: An introduction to the JBC Reviews thematic series. *Journal of Biological Chemistry*, 294(6), 2074–2075. https://doi.org/10.1074/jbc.REV118.006739

Cheng, B. Q., Wei, L. J., Lv, Y. B., Chen, J., & Hua, Q. (2019). Elevating limonene production in oleaginous yeast *Yarrowia lipolytica* via genetic engineering of limonene biosynthesis pathway and optimization of medium composition. *Biotechnology and Bioprocess Engineering*, 24(3), 500–506. https://doi.org/10.1007/s12257-018-0497-9

Deretic, V. (2015). Lipid droplets and their component triglycerides and steryl esters regulate autophagosome biogenesis. *The EMBO Journal*, 34(16), 2111–2113. https://doi.org/10.15252/embj.201592087

Downloaded from https://academic.oup.com/jimb/article/50/1/kuad031/7281721 by guest on 07 November 2023

Finley, D., Ulrich, H. D., Sommer, T., & Kaiser, P. (2012). The ubiquitin-proteasome system of *Saccharomyces cerevisiae*. *Genetics*, 192(2), 319–360. https://doi.org/10.1534/genetics.112.140467

Friedlander, J., Tsakraklides, V., Kamineni, A., Greenhagen, E. H., Consiglio, A. L., MacEwen, K., Crabtree, D. V., Afshar, J., Nugent, R. L., Hamilton, M. A., Shaw, A. J., South, C. R., Stephanopoulos, G., & Brevnova, E. E. (2016). Engineering of a high lipid producing *Yarrowia lipolytica* strain. *Biotechnology for Biofuels*, 9(1), 1–12. https://doi.org/10.1186/s13068-016-0492-3

Fu, J., Zaghen, S., Lu, H., Konzock, O., & Poorinmohammad, N., Kornberg, A., Koseto, D., Wentzel, A., Di Bartolomeo, F., & Kerkhoven, E. J. (2023). Reprogramming *Yarrowia lipolytica* metabolism for efficient synthesis of itaconic acid from flask to semi-pilot scale. *BioRxiv*. https://doi.org/10.1101/2023.07.17.549194

Gajdoš, P., Ledesma-Amaro, R., Nicaud, J. M., Čertík, M., & Rossignol, T. (2016). Overexpression of diacylglycerol acyltransferase in *Yarrowia lipolytica* affects lipid body size, number and distribution. *FEMS Yeast Research*, 16(6), 1–8. https://doi.org/10.1093/femsyr/fow062

Gajdoš, P., Nicaud, J. M., Rossignol, T., & Čertík, M. (2015). Single cell oil production on molasses by *Yarrowia lipolytica* strains overexpressing DGA2 in multicopy. *Applied Microbiology and Biotechnology*, 99(19), 8065–8074. https://doi.org/10.1007/s00253-015-6733-8

Gao, S., Tong, Y., Zhu, L., Ge, M., Jiang, Y., Chen, D., & Yang, S. (2017). Production of β-carotene by expressing a heterologous multifunctional carotene synthase in *Yarrowia lipolytica*. *Biotechnology Letters*, 39(6), 921–927. https://doi.org/10.1007/s10529-017-2318-1

Garbarino, J., Padamsee, M., Wilcox, L., Oelkers, P. M., D'Ambrosio, D., Ruggles, K. V., Ramsey, N., Jabado, O., Turkish, A., & Sturley, S. L. (2009). Sterol and diacylglycerol acyltransferase deficiency triggers fatty acid-mediated cell death. *Journal of Biological Chemistry*, 284(45), 30994–31005. https://doi.org/10.1074/jbc.M109.050443

Gonçalves, F. A. G., Colen, G., & Takahashi, J. A. (2014). *Yarrowia lipolytica* and its multiple applications in the biotechnological industry. *The Scientific World Journal*, 2014, 1–14. https://doi.org/10.1155/2014/476207

Graef, M. (2018). Lipid droplet-mediated lipid and protein homeostasis in budding yeast. *FEBS Letters*, 592(8), 1291–1303. https://doi.org/10.1002/1873-3468.12996

Hapeta, P., Kerkhoven, E. J., & Lazar, Z. (2020). Nitrogen as the major factor influencing gene expression in *Yarrowia lipolytica*. *Biotechnology Reports*, 27, e00521. https://doi.org/10.1016/j.btre.2020.e00521

Hariri, H., Rogers, S., Ugrankar, R., Liu, Y. L., Feathers, J. R., & Henne, W. M. (2018). Lipid droplet biogenesis is spatially coordinated at ER–vacuole contacts under nutritional stress. *EMBO Reports*, 19(1), 57–72. https://doi.org/10.15252/embr.201744815

Hayashi, H. (1995). Pyridoxal enzymes: Mechanistic diversity and uniformity. *The Journal of Biochemistry*, 118(3), 463–473. https://doi.org/10.1093/oxfordjournals.jbchem.a124931

Holkenbrink, C., Dam, M. I., Kildegaard, K. R., Beder, J., Dahlin, J., Doménech Belda, D., & Borodina, I. (2018). EasyCloneYALI: CRISPR/Cas9-based synthetic toolbox for engineering of the yeast *Yarrowia lipolytica*. *Biotechnology Journal*, 13(9), 1–8. https://doi.org/10.1002/biot.201700543

Hunter, T. (1995). Protein kinases and phosphatases: The Yin and Yang of protein phosphorylation and signaling. *Cell*, 80(2), 225–236. https://doi.org/10.1016/0092-8674(95)90405-0

Jacquier, N., Choudhary, V., Mari, M., Toulmay, A., Reggiori, F., & Schneiter, R. (2011). Lipid droplets are functionally connected to the endoplasmic reticulum in *Saccharomyces cerevisiae*. *Journal of Cell Science*, 124(14), 2424–2437. https://doi.org/10.1242/jcs.076836

Kaluzny, M. A., Duncan, L. A., Merritt, M. V., & Epps, D. E. (1985). Rapid separation of lipid classes in high yield and purity using bonded phase columns. *Journal of Lipid Research*, 26(1), 135–140. https://doi.org/10.1016/s0022-2275(20)34412-6

Kerkhoven, E. J., Pomraning, K. R., Baker, S. E., & Nielsen, J. (2016). Regulation of amino-acid metabolism controls flux to lipid accumulation in *Yarrowia lipolytica*. *Npj Systems Biology and Applications*, 2(1), 1–7. https://doi.org/10.1038/npjsba.2016.5

Kevin, B., Rana, S., & Lewis, M. (2022). *Publication-ready volcano plots with enhanced colouring and labeling*.

Koch, B., Schmidt, C., & Daum, G. (2014). Storage lipids of yeasts: A survey of nonpolar lipid metabolism in *Saccharomyces cerevisiae*, *Pichia pastoris*, and *Yarrowia lipolytica*. *FEMS Microbiology Reviews*, 38(5), 892–915. https://doi.org/10.1111/1574-6976.12069

Konzock, O. (2022). *Genetic engineering of Yarrowia lipolytica for the sustainable production of food oils* [Doctoral thesis, Chalmers Tekniska Hogskola, Sweden]. http://proxy.lib.chalmers.se/login?url=https://www.proquest.com/dissertations-theses/genetic-engineering-em-yarrowia-lipolytica/docview/2673036268/se-2?accountid=10041

Konzock, O. & Norbeck, J. (2020). Deletion of MHY1 abolishes hyphae formation in *Yarrowia lipolytica* without negative effects on stress tolerance. *PLoS ONE*, 15(4), 1–11. https://doi.org/10.1371/journal.pone.0231161

Konzock, O., Zaghen, S., Fu, J., & Eduard, J. (2022). Urea is a drop-in nitrogen source alternative to ammonium sulphate in *Yarrowia lipolytica*. *Iscience*, 25(12), 105703. https://doi.org/10.1016/j.isci.2022.105703

Konzock, O., Zaghen, S., & Norbeck, J. (2021). Tolerance of *Yarrowia lipolytica* to inhibitors commonly found in lignocellulosic hydrolysates. *BMC Microbiology*, 21(1), 1–10. https://doi.org/10.1186/s12866-021-02126-0

Law, C. W., Chen, Y., Shi, W., & Smyth, G. K. (2014). Voom: Precision weights unlock linear model analysis tools for RNA-seq read counts. *Genome Biology*, 15(2), 1–17. https://doi.org/10.1186/gb-2014-15-2-r29

Lv, Y., Marsafari, M., Koffas, M., Zhou, J., & Xu, P. (2019). Optimizing oleaginous yeast cell factories for flavonoids and hydroxylated flavonoids biosynthesis. *ACS Synthetic Biology*, 8(11), 2514–2523. https://doi.org/10.1021/acssynbio.9b00193

Magnan, C., Yu, J., Chang, I., Jahn, E., Kanomata, Y., Wu, J., Zeller, M., Oakes, M., Baldi, P., & Sandmeyer, S. (2016). Sequence assembly of *Yarrowia lipolytica* strain W29/CLIB89 shows transposable element diversity. *PLoS ONE*, 11(9), 1–28. https://doi.org/10.1371/journal.pone.0162363

Maleki, F., Ovens, K., Hogan, D. J., & Kusalik, A. J. (2020, June). Gene set analysis: Challenges, opportunities, and future research. *Frontiers in Genetics*, 11, 1–16. https://doi.org/10.3389/fgene.2020.00654

Marella, E. R., Dahlin, J., Dam, M. I., ter Horst, J., Christensen, H. B., Sudarsan, S., Wang, G., Holkenbrink, C., & Borodina, I. (2020, August). A single-host fermentation process for the production of flavor lactones from non-hydroxylated fatty acids. *Metabolic Engineering*, 61, 427–436. https://doi.org/10.1016/j.ymben.2019.08.009

Markham, K. A., Palmer, C. M., Chwatko, M., Wagner, J. M., Murray, C., Vazquez, S., Swaminathan, A., Chakravarty, I., Lynd, N. A., & Alper, H. S. (2018). Rewiring *Yarrowia lipolytica* toward triacetic acid lactone for materials generation. *Proceedings of the National Academy of Sciences*, 115(9), 2096–2101. https://doi.org/10.1073/pnas.1721203115

Downloaded from https://academic.oup.com/jimb/article/50/1/kuad031/7281721 by guest on 07 November 2023

Matthäus, F., Ketelhot, M., Gatter, M., & Barth, G. (2014). Production of lycopene in the non-carotenoid-producing yeast *Yarrowia lipolytica*. *Applied and Environmental Microbiology*, 80(5), 1660–1669. https://doi.org/10.1128/AEM.03167-13

Moldavski, O., Amen, T., Levin-Zaidman, S., Eisenstein, M., Rogachev, I., Brandis, A., Kaganovich, D., & Schuldiner, M. (2015). Lipid droplets are essential for efficient clearance of cytosolic inclusion bodies. *Developmental Cell*, 33(5), 603–610. https://doi.org/10.1016/j.devcel.2015.04.015

Nguyen, T. B., Louie, S. M., Daniele, J. R., Tran, Q., Dillin, A., Zoncu, R., Nomura, D. K., & Olzmann, J. A. (2017). DGAT1-dependent lipid droplet biogenesis protects mitochondrial function during starvation-induced autophagy. *Developmental Cell*, 42(1), 9–21.e5. https://doi.org/10.1016/j.devcel.2017.06.003

Nicaud, J.-M. (2012). *Yarrowia lipolytica*. *Yeast*, 29(10), 409–418. https://doi.org/10.1002/yea.2921

Olzmann, J. A. & Carvalho, P. (2019). Dynamics and functions of lipid droplets. *Nature Reviews Molecular Cell Biology*, 20(3), 137–155. https://doi.org/10.1038/s41580-018-0085-z

Palmer, C. M., Miller, K. K., Nguyen, A., & Alper, H. S. (2020, November). Engineering 4-coumaroyl-CoA derived polyketide production in *Yarrowia lipolytica* through a β-oxidation mediated strategy. *Metabolic Engineering*, 57, 174–181. https://doi.org/10.1016/j.ymben.2019.11.006

Petschnigg, J., Wolinski, H., Kolb, D., Zelling, G., Kurat, C. F., Natter, K., & Kohlwein, S. D. (2009). Good fat, essential cellular requirements for triacylglycerol synthesis to maintain membrane homeostasis in yeast. *Journal of Biological Chemistry*, 284(45), 30981–30993. https://doi.org/10.1074/jbc.M109.024752

Poorinmohammad, N., Fu, J., Wabeke, B., & Kerkhoven, E. J. (2022). Validated Growth Rate-Dependent Regulation of Lipid Metabolism in *Yarrowia lipolytica*. *International Journal of Molecular Sciences*, 23(15), 8517. https://doi.org/10.3390/ijms23158517

Qiao, K., Imam Abidi, S. H., Liu, H., Zhang, H., Chakraborty, S., Watson, N., Kumaran Ajikumar, P., & Stephanopoulos, G. (2015). Engineering lipid overproduction in the oleaginous yeast *Yarrowia lipolytica*. *Metabolic Engineering*, 29, 56–65. https://doi.org/10.1016/j.ymben.2015.02.005

Ritchie, M. E., Phipson, B., Wu, D., Hu, Y., Law, C. W., Shi, W., & Smyth, G. K. (2015). Limma powers differential expression analyses for RNA-sequencing and microarray studies. *Nucleic Acids Research*, 43(7), e47. https://doi.org/10.1093/nar/gkv007

Sandager, L., Gustavsson, M. H., Ståhl, U., Dahlqvist, A., Wiberg, E., Banas, A., Lenman, M., Ronne, H., & Stymne, S. (2002). Storage lipid synthesis is non-essential in yeast. *Journal of Biological Chemistry*, 277(8), 6478–6482. https://doi.org/10.1074/jbc.M109109200

Shi, T., Li, Y., Zhu, L., Tong, Y., Yang, J., Fang, Y., Wang, M., Zhang, J., Jiang, Y., & Yang, S. (2021). Engineering the oleaginous yeast *Yarrowia lipolytica* for β-farnesene overproduction. *Biotechnology Journal*, 16(7), 2100097. https://doi.org/10.1002/biot.202100097

Suda, Y. & Nakano, A. (2012). The yeast Golgi apparatus. *Traffic*, 13(4), 505–510. https://doi.org/10.1111/j.1600-0854.2011.01316.x

Thibault, G. & Ng, D. T. W. (2012). The endoplasmic reticulum-associated degradation pathways of budding yeast. *Cold Spring Harbor Perspectives in Biology*, 4(12), a013193–a013193. https://doi.org/10.1101/cshperspect.a013193

Thomas, P. D. (2017). The gene ontology handbook. *Methods in Molecular Biology*, 1446, 1–9. https://doi.org/10.1007/978-1-4939-3743-1

Väremo, L., Nielsen, J., & Nookaew, I. (2013). Enriching the gene set analysis of genome-wide data by incorporating directionality of gene expression and combining statistical hypotheses and methods. *Nucleic Acids Research*, 41(8), 4378–4391. https://doi.org/10.1093/nar/gkt111

Velázquez, A. P., Tatsuta, T., Ghillebert, R., Drescher, I., & Graef, M. (2016). Lipid droplet-mediated ER homeostasis regulates autophagy and cell survival during starvation. *Journal of Cell Biology*, 212(6), 621–631. https://doi.org/10.1083/jcb.201508102

Wang, J., Ledesma-Amaro, R., Wei, Y., Ji, B., & Ji, X. J. (2020, May). Metabolic engineering for increased lipid accumulation in *Yarrowia lipolytica*—A review. *Bioresource Technology*, 313, 123707. https://doi.org/10.1016/j.biortech.2020.123707

Zeng, S. Y., Liu, H. H., Shi, T. Q., Song, P., Ren, L. J., Huang, H., & Ji, X. J. (2018). Recent advances in metabolic engineering of *Yarrowia lipolytica* for lipid overproduction. *European Journal of Lipid Science and Technology*, 120(3), 1700352. https://doi.org/10.1002/ejlt.201700352

Received: August 15, 2023. **Accepted:** September 19, 2023

© The Author(s) 2023. Published by Oxford University Press on behalf of Society of Industrial Microbiology and Biotechnology. This is an Open Access article distributed under the terms of the Creative Commons Attribution License (https://creativecommons.org/licenses/by/4.0/), which permits unrestricted reuse, distribution, and reproduction in any medium, provided the original work is properly cited.

Downloaded from https://academic.oup.com/jimb/article/50/1/kuad031/7281721 by guest on 07 November 2023